Electromagnetic Propagation in Four-Layered Media Due to a Vertical Electric Dipole: A Clarification

J. D. Cross and P. R. Atkins

***Abstract*—This communication presents a quasi-analytical method for predicting the electromagnetic propagation in four-layered media due to a vertical electric dipole. The method includes the components known as the direct, ideal reflected, lateral, and trapped surface waves. Previous literature, studying less complex geometries, is extensively reviewed and found to be incomplete and inaccurate in a number of places. These deficiencies are highlighted and the methodology is presented with enough detail to allow repetition of the results. Results are shown which approximate the scenario of a leaking water-pipe, buried in the shallow sub-surface. It is shown that the trapped surface wave does not dominate in this scenario. Furthermore, it is shown that the trapped surface wave magnitude is reduced when conductivity of the fourth layer is reduced, or when the third layer thickness is increased; these results fit the qualitative expectation based on previous results.**

***Index Terms*—Dielectric waveguides, dipole antennas, electromagnetic propagation in absorbing media, surface waves.**

I. Introduction

This work demonstrates a quasi-analytical method for calculating the electromagnetic (EM) field due to a vertical electric dipole (VED) in four-layered media. For example, if a water pipe is leaking in the shallow sub-surface, the simplest applicable model is one with four layers (Fig. 1). A similar argument can be constructed when considering a large air-void, mineral deposit, or buried utility.

The EM field in stratified media is the subject of a large body of research [1]. Previous researchers have proposed a number of analyses, including a four-layered geometry where the fourth layer is perfectly conductive [2]–[8]. However, this research has not been without controversy, and the contribution of the trapped surface wave to the EM field was only recently evaluated for a three-layered geometry [5].

An analytical model for the EM field in this geometry is useful for several reasons: A numerical solution converges slowly due to the highly oscillatory nature of the integral equations describing the EM field in this geometry; a horizontal-electric dipole which could model an in-pipe excitation is a logical extension of the VED case [9]; and when designing systems, it is useful to be able to quickly adjust model parameters—something that cannot be achieved with a slow numerical solution.

A quasi-analytical solution to the integral equations describing the EM field in layered media, due to a VED presented by [10], is presented. The solution relies on numerical root finding algorithms and the far-field solution, but is otherwise analytical. It is shown that a number of flaws existed in previous publications [5]–[7]. These flaws have made repeating earlier results exceedingly difficult and the requirement to correct previous errors makes this work quite involved. The derivations are limited to the methodology proposed by [2], and developed by [5]–[8], while the geometry is illustrated in Fig. 2. This work assumes that each layer is homogenous, anisotropic, and linear; that the far-field assumption is valid at the observation point; that the lateral wave is dominated by the contribution of the first branch cut which allows single values for the wavenumber of the lateral wave, and an approximate value for the Hankel function; finally, it is assumed that the Fresnel integral may be accurately approximated using the McLaurin series expansion of the error-function.

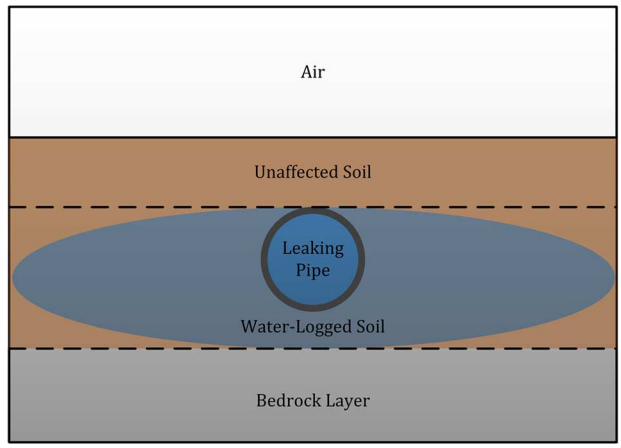

Fig. 1. Geological profile of a leaking pipe. A four-layered model represents the simplest approximation of this geometry.

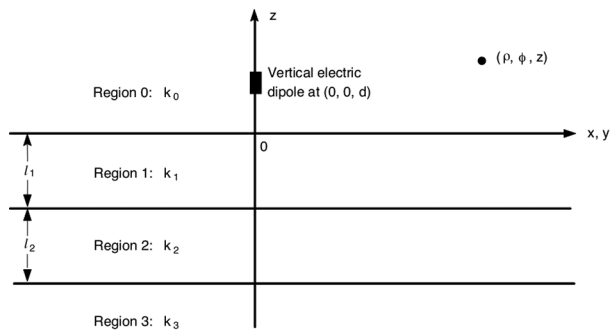

Fig. 2. System Geometry [7] 2008 EMW Publishing.

This communication is structured as follows: The underlying integral equations, defined by King *et al.* [10], and utilized in the three-layer scenario by [2] are stated. The analysis required to solve these integral equations is then presented. Previous research, which led to this analysis, is then summarized and the errors and omissions therein described. Example results are given for the leaking pipe scenario illustrated in Fig. 1.

II. Method

The EM field in layered media is described by (1) and two equivalent equations [6], [10]:

$$B_{0\phi}(\rho,z)=\frac{i\mu_0}{4\pi}\int_0^\infty\Big[e^{i\gamma_0|z-d|}+e^{i\gamma_0(z+d)}-(Q+1)e^{i\gamma_0(z+d)}\Big]\gamma_0^{-1}J_1(\lambda\rho)\lambda^2 d\lambda \quad (1)$$

where i is the square-root of -1; μ_0 is the permeability of free space; z and d refer to the position of the observation point and dipole, respectively; Q is a gathering of terms, defined below, $J1$ is the Bessel

Manuscript received November 21, 2013; revised June 18, 2014; accepted October 31, 2014. Date of publication December 18, 2014; date of current version January 30, 2015. This work was supported by the U.K. Engineering and Physical Sciences Research Council under grant EP/F065965/1.

The authors are with the Department of Electronic, Electrical and Computer Engineering, University of Birmingham, Birmingham B15 2TT, U.K. (e-mail: p.r.atkins@bham.ac.uk).

Color versions of one or more of the figures in this communication are available online at http://ieeexplore.ieee.org.

Digital Object Identifier 10.1109/TAP.2014.2384035

function of the first kind, of order 1; λ is the wavelength; and γ_0 is the propagation constant of region 0:

$$\gamma_j = \sqrt{k_j^2 - \lambda^2} \tag{2}$$

where k_j is the wavenumber in region j:

$$k_j = \omega\sqrt{\mu_0(\varepsilon_0\varepsilon_j + i\sigma_j/\omega)} \tag{3}$$

where ω is the angular frequency (rads s^{-1}), ε_0 is the permittivity of free space, ε_j is the relative-permittivity of region j, and σ_j is the electrical conductivity of region j (S m^{-1}).

It is well known that the solution to (1), and its equivalents, may be separated into the direct, ideal reflected, lateral, and trapped-surface waves [5]–[7].

A. Direct and Ideal Reflected Waves

The direct wave is the wave which propagates through air from the VED to the observation point, and the ideal-reflected wave is that which propagates via a single reflection off the surface. Both terms are independent of the composition of the media, and so previous solutions are used:

$$B_{0\phi}^{(1)} = -\frac{\mu_0}{4\pi}e^{ik_0 r_1}\left(\frac{\rho}{r_1}\right)\left(\frac{ik_0}{r_1} - \frac{1}{r_1^2}\right) \tag{4}$$

$$B_{0\phi}^{(2)} = -\frac{\mu_0}{4\pi}e^{ik_0 r_2}\left(\frac{\rho}{r_2}\right)\left(\frac{ik_0}{r_2} - \frac{1}{r_2^2}\right) \tag{5}$$

where (1) and (2) denote the direct, and ideal reflected waves, respectively; r_1 and r_2 denote the cylindrical coordinate descriptions for the path lengths:

$$r_1 = \sqrt{\rho^2 + (z-d)^2} \tag{6}$$

$$r_2 = \sqrt{\rho^2 + (z+d)^2}. \tag{7}$$

B. Derivation of Q

The Q term was first used by [10] as a gathering of terms for a larger integral equation, consequently it does not have a physical definition. The term for Q in an n-layered half space is defined as:

$$-Q_n = \frac{\gamma_0 - \frac{k_0^2}{\omega\mu_0}Z_{s0}(0)}{\gamma_0 + \frac{k_0^2}{\omega\mu_0}Z_{s0}(0)} \tag{8}$$

where $z_{so}(0)$ is the surface impedance (Ohms), derived by King *et al.* [10]. In a four-layered medium, $z_{so}(0)$ is given by:

$$Z_{s0} = \frac{\omega\mu_0\gamma_1}{k_1^2}\tanh\left[-i\gamma_1 l_1 + \tanh^{-1}\left[\left(\frac{\gamma_2 k_1^2}{\gamma_1 k_2^2}\right)\tanh\left[-i\gamma_2 l_2 + \tanh^{-1}\left(\frac{\gamma_3 k_2^2}{\gamma_2 k_3^2}\right)\right]\right]\right]. \tag{9}$$

By substituting (9) into (8), using trigonometric identities to express the hyperbolic tangent and inverse hyperbolic tangent function in terms of tangents, and gathering like terms in the fraction, $Q+1$ may be expressed as [11]:

$$Q + 1 = \frac{2ik_0^2\gamma_1 A(\lambda)}{q(\lambda)} \tag{10}$$

where:

$$A(\lambda) = -\frac{i\gamma_1\gamma_3 k_2^2\tan(\gamma_1 l_1)\tan(\gamma_2 l_2)}{k_1^2} + i\gamma_2\gamma_3 + \frac{\gamma_2^2 k_3^2\tan(\gamma_2 l_2)}{k_2^2} + \frac{\gamma_1\gamma_2 k_3^2\tan(\gamma_1 l_1)}{k_1^2} \tag{11}$$

$$q(\lambda) = \frac{\gamma_0\gamma_2^2 k_1^2 k_3^2\tan(\gamma_1 l_1)\tan(\gamma_2 l_2)}{k_2^2} - \gamma_0\gamma_1\gamma_2 k_3^2 - \gamma_0\gamma_1\gamma_2 k_3^2 + i\gamma_0\gamma_2\gamma_3 k_1^2\tan(\gamma_1 l_1) + i\gamma_0\gamma_1\gamma_3 k_2^2\tan(\gamma_2 l_2) + \frac{\gamma_1^2\gamma_3 k_0^2 k_2^2\tan(\gamma_1 l_1)\tan(\gamma_2 l_2)}{k_1^2} - \gamma_1\gamma_2\gamma_3 k_0^2 + \frac{i\gamma_1\gamma_2^2 k_0^2 k_3^2\tan(\gamma_2 l_2)}{k_2^2} + \frac{i\gamma_1^2\gamma_2 k_0^2 k_3^2\tan(\gamma_1 l_1)}{k_1^2}. \tag{12}$$

C. Separation of Lateral and Trapped Surface Waves

Considering (1) as the summation of the different wave paths, the direct and ideal reflected waves are defined by (4) and (5); the remaining terms are defined by (13), additionally the Bessel function is replaced with the Hankel function to extend the integral bounds to $-\infty$:

$$B_{0\varphi}^{(3)} = \frac{\mu_0 k_0^2}{4\pi}\int_{-\infty}^{\infty}\frac{A(\lambda)}{q(\lambda)}\frac{\gamma_1 e^{i\gamma_0(z+d)}H_1^{(1)}(\lambda\rho)\lambda^2}{\gamma_0}d\lambda. \tag{13}$$

As with [5]–[7], (13) is solved using complex analysis which allows the integral to be separated into the sum of the residues and a contour integral in the complex plane [12]:

$$B_{0\phi}^{(3)} = -\frac{ik_0^2\mu_0}{4\pi}\left\{2\pi i\times\Sigma_j\, Residues\,(\lambda_j^*) + \Sigma_k\int_{\Gamma_k}\frac{A(\lambda)}{q(\lambda)\gamma_0}\gamma_1 e^{i\gamma_0(z+d)}H_1^{(1)}(\lambda\rho)\lambda^2 d\lambda\right\} \tag{14}$$

where λ_j^* refers to the poles in the integrand in (13), and $\angle_k$ refers to the branch cuts in the complex plane. The contour integral refers to the lateral wave, while the sums of residues refers to the trapped surface wave; the following two sections show the evaluation of these terms.

D. Lateral Wave

It was argued by [6], when extending the work of [5], that the lateral wave component in the lowest layer is negligible if the lowest layer is slightly conductive. This argument is extended here, and so the definition of the lateral wave for a four-layered media with perfectly conductive fourth layer [7] is used. The expression relies on the Fresnel integral, which is approximated using the error-function and its McLaurin series expansion [13]:

$$B_{0\phi}^{(3L)} = -\frac{\mu_0 k_0^3}{2}\sqrt{\frac{1}{\pi k_0\rho}}e^{ik_0 r_2}e^{-ip^*}\times F(p^*)\frac{\gamma_{10}\gamma_{20}\tan(\gamma_{20}l_2) + \frac{k_2^2}{k_1^2}\gamma_{10}^2\tan(\gamma_{10}l_1)}{\gamma_{10}k_2^2 - \gamma_{20}k_1^2\tan(\gamma_{10}l_1)\tan(\gamma_{20}l_2)} \tag{15}$$

where $F(p^*)$ is the Fresnel integral:

$$F(p^*) = \frac{1}{2}(1+i) - \int_0^{p^*}\frac{e^{it}}{\sqrt{2\pi t}}dt \tag{16}$$

$$p^* = \frac{k_0\rho}{2}\left[\frac{z+d}{\rho} + i\frac{k_0}{k_1^2}\gamma_{10}\cdot\frac{\gamma_{10}k_2^2\tan(\gamma_{10}l_1) + \gamma_{20}k_1^2\tan(\gamma_{20}l_2)}{\gamma_{10}k_2^2 - \gamma_{20}k_1^2\tan(\gamma_{10}l_1)\tan(\gamma_{20}l_2)}\right]^2. \tag{17}$$

Use of the far-field assumption allows simplification of the propagation terms, as follows:

$$\gamma_1 \approx \gamma_{10} = \sqrt{k_1^2 - k_0^2}, \tag{18}$$

$$\gamma_2 \approx \gamma_{20} = \sqrt{k_2^2 - k_0^2}. \tag{19}$$

E. Trapped Surface Wave

1) Calculation of the Poles: The poles in the integrand of (13) occur when the function $q(\lambda) = 0$. Considering (12), an analytical solution for the zeros in $q(\lambda)$ was deemed unfeasible. Therefore, a numerical simplex search was implemented [14], this was found to be considerably more stable than the Newton-Raphson method used by [6], [7]. The values for the poles are included in the results section; without these, repetition or validation of this work is difficult.

2) Evaluation of the Residues: The residue of the division of two functions, at a pole z_0 is given by (20), which is not mathematically complete but suffices for this work. Substituting (20) into (14) gives the expression for the trapped surface wave (21). In common with other equations presented here, this is cumbersome but presents no obstacle for a software package such as MATLAB or Mathematica

$$Res\left[\frac{f(z)}{g(z)}, Z_0\right] = \frac{f(z_0)}{g'(z_0)}, \tag{20}$$

$$\begin{aligned} B_{0\phi}^{(3T)} &= 2\pi i \times -\frac{ik_0^2\mu_0}{4\pi} \\ &\times \Sigma_j \frac{A\left(\lambda_j^*\right)}{\frac{d}{d\lambda}\left[q\left(\lambda_j^*\right)\right]\gamma_0\left(\lambda_j^*\right)} \gamma_1 e^{i\gamma_0(z+d)} H_1^{(1)} \\ &\times \left(\left(\lambda_j^*\right)\rho\right)\left(\lambda_j^*\right)^2. \end{aligned} \tag{21}$$

III. Errors in Previous Publications

It is hoped that Section II allows repetition of this work, without recourse to a significant number of other references. However, a number of errors and omissions have been noted in the preceding literature which obscure the best method for repeating previous measurements, or are highly misleading. The errors are discussed in chronological order:

1) Roots of $q(\lambda)$ Given by [5] are Misleading: The method presented by [5] for calculating the roots of $q(\lambda)$ makes the assumption that the roots are real—this assumption is not always valid. Furthermore, the figures presented by [5] show the "first root" of $q(\lambda)$ which is insufficient to reproduce the final results. Fig. 3 shows the results presented by [5], while Fig. 4 shows all of the calculated roots.

2) Sign Error in Equations 9–11 of [5]: The equation for Q is not given by [5], which makes repeating their results challenging. However, a sign error is present in the equations for the lateral and trapped surface wave given by [5]. The supporting derivation is shown in [11].

3) Graphs Showing Roots of $q(\lambda)$ by [6] are Erroneous: Results for the first root of $q(\lambda)$ are presented by [6]. The difficulties in calculating the roots of an unstable, complex function are discussed above, but the graphs presented by [6] have been found to be incomplete. It is known that the real component of the propagation constant, γ, cannot be negative [10]. However, the only way to reproduce the results from [6] is to allow the propagation constant to be negative

4) Graphs Showing Roots of $q(\lambda)$ by [7] are Erroneous: One of the most challenging parts of repeating the work published by previous authors is the determination of the roots of $q(\lambda)$. After repeating the calculations by [7] for the roots of $q(\lambda)$, it has been concluded that the graphs presented were erroneous and were computed using different input parameters to those stated. This conclusion is supported by comparing similar results by [8] which were very close to those calculated in this work but do not resemble the results by [7].

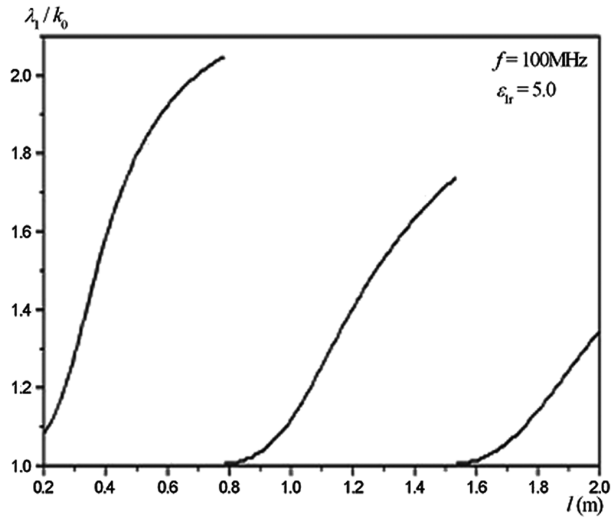

Fig. 3. The first root of $q(\lambda)$ with increasing layer thickness, l. When compared with Fig. 4 this figure is seen to be incomplete and has not always selected the "first" root. After [5] 2002 by the AGU.

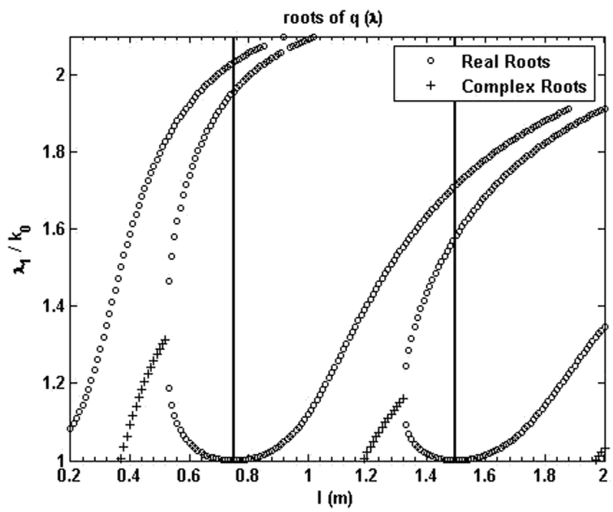

Fig. 4. Roots $q(\lambda)$ calculated using equations derived by [5]. All roots are shown, including complex roots not calculable with the method presented by [5]. All roots are required to evaluate the trapped surface wave.

5) EM Field Results by [7] are Excessively Filtered: The results presented by [7] for the total field could not be replicated. The fields due to the direct, reflected, and lateral (DRL) waves agree. However, the trapped surface wave has much less of a contribution than shown by [7]. Furthermore, the figure showing the total field magnitude appears to have been smoothed to the point of being misleading. The graph presented by [7] is shown in Fig. 5 while the result computed for this work is shown in Fig. 6.

IV. Results

Results are presented which approximate a leaking, buried, pipe. The layers are, respectively, air, dry soil ($\varepsilon_r = 4$, thickness = 1 meter), air (thickness $= 0.01$ meter), and water-logged soil ($\varepsilon_r = 4$, $\sigma = 4$). The direct and ideal-reflected waves were calculated using (4) and (5), the lateral wave was calculated using (15)–(20). Poles for the function

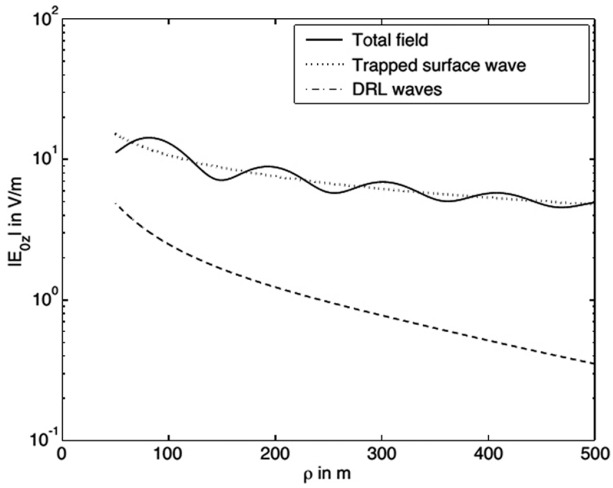

Fig. 5. The total field calculated by Xu et al. [7] in a four layered medium with a perfectly conductive fourth layer. Where $f = 100$ MHz, $\boldsymbol{\varepsilon}_{1r} = 2.65$, $\boldsymbol{\varepsilon}_{2r} = 2.65$, $k1l1 = k2l2 = 0.3$, and $z = d = 0$.

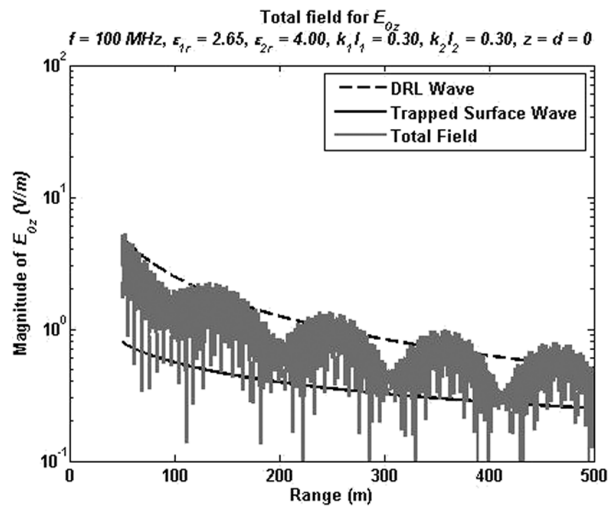

Fig. 6. The total field calculated using the technique described by [7]. When comparing to Fig. 5, significant smoothing is evident.

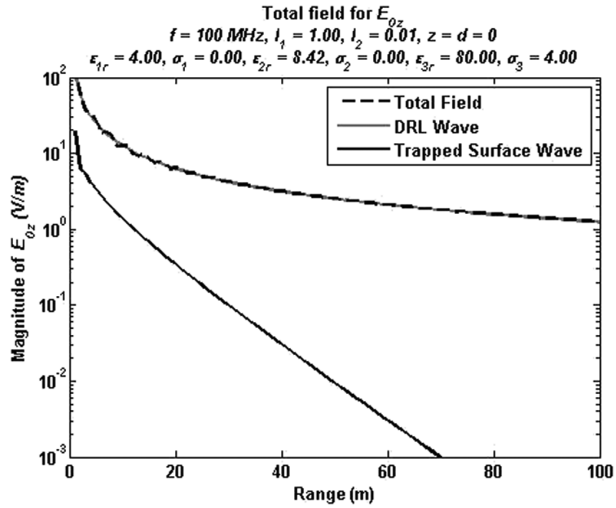

Fig. 7. Magnitude of the E_{0z} field component in the described geometry. The trapped surface wave contributes negligibly to the total field.

$q(\lambda)$ were found at $\lambda = 4.9659 + 1.8750i$ and $\lambda = 2.9048 + 1.6585i$, which allowed the calculation of the trapped surface wave using (22). The predicted EM field at increasing range from the VED is shown in Fig. 7.

None of the results calculated for this work showed significant contribution to the overall field from the trapped surface wave. Qualitatively, this can be explained by the dominant contribution being located at the deepest boundary where the field contribution must pass two other boundaries to contribute to the measured field. Based on these results, it seems likely that the contribution of the trapped surface wave will decrease as the number of layers increases, in the situation where the most conductive layer remains the deepest. Results also confirmed the qualitative assessment that the trapped surface wave is more efficiently excited with increased conductivity of the fourth layer, and reduced thickness of the third layer.

V. Conclusions

The derivation of the electromagnetic field due to a vertical electric dipole in four layered geometries has been derived. The method for this derivation has been presented in a way which allows the reader to define their own geometries and compute results without reference to large numbers of other works.

Several errors in previously published works have been found and explained, these errors made repeating previous works extremely challenging. Errors included sign errors in equations, graphs plotted using parameters different to those stated, and incomplete results for the derivation of the trapped surface wave.

The derivations required for these results are unwieldy, and it is strongly recommended future researchers take great care to guard against algebraic errors which are easily made and only found with great difficulty.

An example result has been presented, which is illustrative of the power of a solution to the problem of the electromagnetic field due to a vertical electric dipole in a four-layered structure, when considering buried objects or leaking utilities. It has been shown that the trapped surface wave is negligible in the scenarios presented. In common with the findings for geometries with fewer layers, high conductivity in the lowest layer increases the contribution by the trapped surface wave. But these results suggest that an increase the number of layers in a geometry acts to reduce the contribution of the trapped surface wave.

References

[1] J. R. Wait, "The ancient and modern history of EM ground-wave propagation," *IEEE Antennas Propag. Mag.*, vol. 40, pp. 7–24, 1998.

[2] R. W. P. King and S. S. Sandler, "The electromagnetic field of a vertical electric dipole in the presence of a three-layered region," *Radio Sci.*, vol. 29, pp. 97–113, 1994.

[3] J. R. Wait, R. W. P. King and S. S. Sandler, Eds., "Comment on The electromagnetic field of a vertical electric dipole in the presence of a three-layered region," *Radio Sci.*, vol. 33, pp. 251–253, 1998.

[4] R. W. P. King and S. S. Sandler, "Reply," *Radio Sci.*, vol. 33, pp. 255–256, 1998.

[5] H. Q. Zhang and W. Y. Pan, "Electromagnetic field of a vertical electric dipole on a perfect conductor coated with a dielectric layer," *Radio Sci.*, vol. 37, pp. 13-1–13-7, 2002.

[6] H. Q. Zhang *et al.*, "The electromagnetic field of a vertical dipole on the dielectric-coated imperfect conductor," *J. Electromagn. Waves Applicat.*, vol. 18, pp. 1305–1320, 2004.

[7] Y. H. Xu *et al.*, "Trapped surface wave and lateral wave in the presence of a four-layered region," *Progr. Electromagn. Res.*, vol. 82, pp. 271–285, 2008.

[8] K. Li, *Electromagnetic Fields in Stratified Media*. Hangzhou, China: Zhejiang University Press, 2009.

[9] Y. L. Lu *et al.*, "Electromagnetic field of a horizontal electric dipole buried in a four-layered region," *Progr. Electromagn. Res.*, vol. 16, pp. 247–275, 2009.
[10] R. W. P. King *et al., Lateral Electromagnetic Waves: Theory and Applications to Communications, Geophysical Exploration, Remote Sensing*. Berlin: Springer, 1992.
[11] J. D. Cross, "Low-frequency electromagnetic fields for the detection of buried objects in the shallow sub-surface," Ph.D. dissertation, Electron., Elec., Comp. Engrg., Univ. Birmingham, Birmingham, U.K., 2014.
[12] J. D. Paliouras and D. S. Meadows, *Complex Variables for Scientists and Engineers*, 2nd ed. New York, NY, USA: Macmillan, 1990.
[13] E. Kreyszig *et al., Advanced Engineering Mathematics*, 8th ed. New York, NY, USA: Wiley, 1999.
[14] J. Lagarias *et al.*, "Convergence properties of the Nelder–Mead simplex method in low dimensions," *SIAM J. Optim.*, vol. 9, pp. 112–147, 1998.

Substrate Integrated Magneto-Electric Dipole Antenna for 5G Wi-Fi

Hau Wah Lai and Hang Wong

***Abstract*—In this communication, a new technique—tapered H-shaped ground, is proposed to reduce the thickness of a magneto-electric (ME) dipole antenna. By employing the proposed technique, the antenna height of the ME dipole antenna is reduced from 0.25 to 0.11 λ_0 (where λ_0 is the wavelength of 5.5 GHz). This new antenna structure can be easily realized by the multi-layer printed circuit board (PCB) technology, which is low cost and easy to fabricate. Measured results show that this antenna has an impedance bandwidth of 18.74% for $\mathrm{VSWR} \leq 2$ (4.98 to 6.01 GHz). Stable radiation patterns with low back radiation and low cross polarization radiation are achieved across the entire operating bandwidth for 5G Wi-Fi.**

***Index Terms*—Magneto-electric dipole, low profile, low back radiation, low cross polarization, 5G Wi-Fi.**

I. Introduction

5G Wi-Fi becomes very popular in recent wireless communications. Its operating frequency is between 5.15 and 5.875 GHz. A lot of literatures show that magneto-electric (ME) dipole antennas can be applied to different kinds of wireless communications, such as base station antennas for mobile communications [1]–[4], ultra wideband systems [5] and millimetre-wave radio [6] due to their excellent electrical characteristics, including wide bandwidth, low back radiation and symmetrical radiation patterns over the entire operating frequencies. However, the disadvantage of these conventional ME-dipoles is high profile, which is $0.25\lambda_0$. In order to reduce the height, using folded structures [7]–[9] or loaded with dielectric materials [10] were proposed. Although these antennas [7]–[10] have low-profile and wideband characteristics, they are difficult in realization when they operate at high frequencies. The antenna size will become smaller when the operating frequency is higher. Especially for the antenna design in [10], it is hard to integrate the Γ-shaped feeding probes and the dielectric substrate block properly within a tiny size.

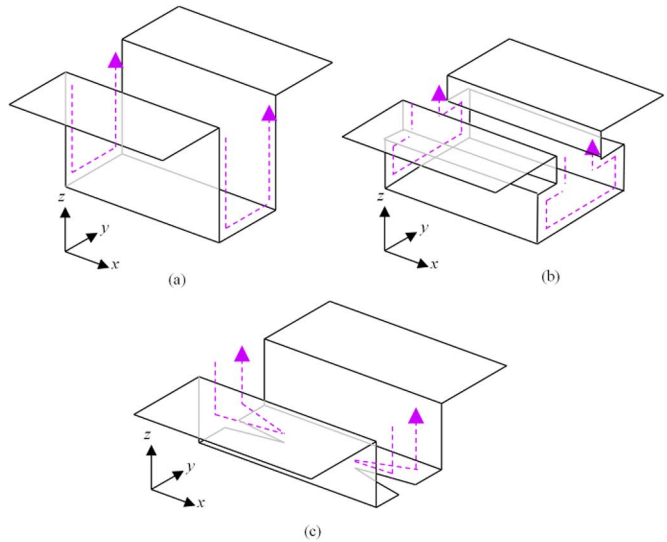

Fig. 1. Vertical current direction of (a) conventional ME dipole antenna, (b) ME dipole antenna with folded parallel walls structure in [7] and [8], (c) proposed ME dipole antenna with H-shape ground.

In this communication, a technique named tapered H-shaped ground is proposed for a ME dipole antenna. By applying this approach, the thickness of the ME dipole antenna can be highly reduced from 0.25 to 0.11 λ_0. The proposed methodology can be easily realized by stacking several PCB layers. It is well-known that PCB fabrication is low-cost, reliable and simple. In this work, the electric dipole is generated from the horizontal dipole arms. The magnetic dipole is induced by the help of the two open slots printed on the H-shaped ground. The current distribution of the magnetic dipole is folded on the ground plane after introducing the two open slots on the H-shaped ground. To further reduce the back radiation, a reflector is added at the bottom layer of the antenna. The proposed antenna has an impedance bandwidth of 18.74% ($\mathrm{VSWR} \leq 2$), which is from 4.98 to 6.01 GHz. The radiation pattern of the antenna has low back radiation, low cross polarization level and stable radiation patterns across its operating bandwidth. The peak gain of the antenna is 6.8 dBi.

II. Principle of the Proposed Methodology

The design of a ME dipole antenna in [1] is a combination of a half wavelength electric dipole and a quarter-wavelength patch antenna. For the height of the ME dipole antenna, it is equal to the length of the quarter-wavelength patch. Therefore, shorten the physical length of the quarter-wavelength patch means reducing the height of the ME dipole antenna. Folding the parallel walls into different shapes along the z-axis [7]–[9] can achieve this goal. An example of the folding technique is shown in Fig. 1(b). However, this approach is hard to fabricate. To fold a metal plate into multiple sections is challenging. In this communication, it is found that the current direction can be folded along the x axis and the fabrication process can be simplified. It can be done by cutting a pair of slots on the ground plane. A tapered H-shape ground plane is

Manuscript received March 12, 2014; revised October 06, 2014; accepted December 08, 2014. Date of publication December 18, 2014; date of current version January 30, 2015. This work was supported in part by the Research Grants Council of the Hong Kong SAR, China (Project No. CityU 138413), the Fundamental Research Program of Shenzhen City(Grant No. JCYJ20140509155229810) and in part by the National Science Foundation of China(Grant No. 61372056).

The authors are with the State Key Laboratory of Millimeter Waves and Department of Electronic Engineering, City University of Hong Kong, Hong Kong SAR (e-mail: hang.wong@cityu.edu.hk).

Color versions of one or more of the figures in this communication are available online at http://ieeexplore.ieee.org.

Digital Object Identifier 10.1109/TAP.2014.2384015